Carbohydrate Polymers 123 (2015) 46–52

Contents lists available at ScienceDirect

Carbohydrate Polymers

journal homepage: www.elsevier.com/locate/carbpol

^{1}H NMR and ^{1}H–^{13}C HSQC surface characterization of chitosan–chitin sheath-core nanowhiskers

Antonio G.B. Pereira[a,b], Edvani C. Muniz[a], You-Lo Hsieh[b,*]

[a] Grupo de Materiais Poliméricos e Compósitos (GMPC), Department of Chemistry, Maringá State University, Av. Colombo, 5790, 87020-900 Maringá, Paraná, Brazil
[b] Fiber and Polymer Science, University of California, Davis, One Shields Avenue, Davis, CA 95616, USA

ARTICLE INFO

Article history:
Received 20 October 2014
Received in revised form
31 December 2014
Accepted 2 January 2015
Available online 16 January 2015

Keywords:
NMR spectroscopy
Nanowhiskers
Chitin
Chitosan
Surface deacetylation

ABSTRACT

Surface deacetylation of chitin nanowhiskers (CtNWs) to chitosan–sheath/chitin-core nanowhiskers (CsNWs) was successfully monitored by liquid-state high-resolution NMR of colloidal suspensions of these never-dried nanowhiskers. CtNWs were derived from acid hydrolysis (3 N HCl, 30 mL/g, 90 min, 104 °C) of chitin at 65% yield and 86% *CrI*. Deacetylation (50% NaOH, 48 h, 50 °C) of CtNWs generated CsNWs with unchanged nanowhisker morphology and overall length and width dimensions, but a reduced *CrI* of 54%. Successful step-wise exchanging the aqueous media with acetone, then D_2O prevented agglomeration of nanowhiskers and enabled NMR detection of individual nanowhiskers. The crystalline structure of CtNWs and CsNWs provided different chemical environments for the glucosamine hydrogen atom H2, splitting the NMR signals into 2 peaks (δ 3.0 and δ 3.35 ppm) which differed from that reported for soluble chitosan (δ 3.2 ppm). Besides, ^{1}H–^{13}C HSQC was only possible for CsNWs indicating the NMR phenomenon observed to represent that of the surfaces where the outer layers were highly mobile and less crystalline. The degree of acetylation at the surfaces was determined from ^{1}H NMR data to be 56% and 9% for CtNWs and CsNWs, respectively.

1. Introduction

Nanomaterials with at least one dimension that is less than 100 nm (Balogh, 2010) have shown to exhibit distinctly unique physical, biological and chemical properties from those of the same chemical constituents but at macro-scale dimensions (Bhattacharya & Mukherjee, 2008; Xia, Xiong, Lim, & Skrabalak, 2009). Irrespective of their shapes (nanospheres, nanoplates, nanorods, *etc.*), the majority of nanomaterials reported to date have been based on either carbon or metals, including carbon nanotube, graphene, noble metals (*e.g.*, Au, Ag, *etc.*) and metal oxides, that demand expensive precursors, toxic reducing agents and high energy input as well as other environmental and health concerns (Faramarzi & Sadighi, 2013; Thakkar, Mhatre, & Parikh, 2010).

More recently, natural polymeric nanomaterials have been increasingly studied as good candidates in place of carbon and metallic nanomaterials in many applications. Natural polymer based nanomaterials have numerous advantages, including low density, low cost, vast availability, straightforward production, renewability and sustainability (biodegradability, non toxicity, *etc.*). Among them, nanocellulose has been the most intensively studied. Nanomaterials based on chitin, the second most available polysaccharide in the biosphere, on the other hand, are far less investigated. Chitin, β(1 → 4)-linked *N*-acetyl-β-D-glucosamine, most commonly found in arthropods, nematodes and fungi (Rinaudo, 2006), is highly crystalline in its native form, *i.e.*, typically over 70% crystalline depending on sources (Cárdenas, Cabrera, Taboada, & Miranda, 2004), and can be processed into highly crystalline nanoparticles or nanowhiskers (Zeng, He, Li, & Wang, 2011). Chitin nanowhiskers (CtNWs) have been derived through acid hydrolysis (Marchessault, Morehead, & Walter, 1959; Paillet & Dufresne, 2001) while longer fibrils could be generated by 2,2,6,6-tetramethylpiperidine-1-oxyl radical (TEMPO) mediated oxidation followed by mechanical disintegration of chitin (Fan, Saito, & Isogai, 2007) or by surface cationization followed by mechanical defibrillation (Fan, Saito, & Isogai, 2010).

Despite all the desirable nano-dimensional attributes of nanocellulose and chitin nanowhiskers, the abundant surface polar groups cause nanocellulose and chitin nanowhiskers to aggregate upon drying, losing their unique individual nano-domain features (Jiang & Hsieh, 2013). Other than wet chemistry techniques applicable to aqueous media, characterization of these polysaccharide

* Corresponding author. Tel.: +1 530 752 0843; fax: +1 530 752 7584.
E-mail address: ylhsieh@ucdavis.edu (Y.-L. Hsieh).

http://dx.doi.org/10.1016/j.carbpol.2015.01.017
0144-8617/

nanocrystals is limited to that of aggregated solids rather than individual nanowhiskers. For instance, freeze-dried chitin nanowhisker solids have been analyzed by solid state ^{13}C NMR to be similar to that of isolated chitin powder (Fan, Saito, & Isogai, 2009; Goodrich & Winter, 2006; Huang, Zhang, Yang, Zhang, & Xu, 2013). Highly deacetylated (over 95%) chitin whiskers have been analyzed by ^{1}H NMR (Lertwattanaseri, Ichikawa, Mizoguchi, Tanaka, & Chirachanchai, 2009; Phongying, Aiba, & Chirachanchai, 2006; Phongying, Aiba, & Chirachanchai, 2007). However, ^{1}H NMR spectra were that of soluble chitosan in deuterium chloride (DCl) or deuterated acetic acid (CD_3COOD), not individual nanowhiskers, since chitosan is soluble in acidic conditions. To truly characterize chitin or chitosan nanowhiskers individually, these nanodomains must remain in isolated individual forms to allow liquid phase NMR analysis.

This paper reports, for the first time, the acquisition of ^{1}H NMR and ^{13}C NMR data from never-dried suspensions of chitin/chitosan nanocrystals by solvent exchange thus avoiding potential structural alteration or dissolution of nanocrystals from the use of deuterated acid. Chitosan-sheath chitin-core nanowhiskers (CsNWs) were obtained by surface deacetylation of chitin nanowhiskers (CtNWs) and such surface chemical modification was monitored through liquid-state high-resolution NMR to provide new insights in the chemical structures of chitin/chitosan nanocrystal surfaces. These liquid phase NMR techniques offer new analytical capability to detect structural changes and modification of chitin/chitosan nanowhiskers for process and product development.

2. Experimental

2.1. Materials and methods

Chitin (CT, CAS 1398-61-4) from crab shells was purchased from Sigma (St. Louis, MO, USA). Potassium hydroxide (85%, EM Science, CAS 1310-58-3), sodium hydroxide (97%, EMD, CAS 1310-73-2), hydrochloric acid (36.5%, EMD, CAS 7647-01-0), pH 4 acetate buffer (15% sodium acetate and 48% acetic acid w/v, VWR), sodium chlorite (80%, Alfa Aesar, CAS 7758-19-2) were used without further purification. Purified water (Millipore – Milli-Q^{TM} Water System) was used in all experiments. All aqueous solutions were prepared in w/v% unless specified.

2.2. Chitin purification and hydrolysis

Chitin was purified from crab shell chitin by removing residual proteins and bleaching as previously reported (Paillet & Dufresne, 2001; Pereira, Muniz, & Hsieh, 2014). Proteins were removed by heating 5 g of chitin in 150 mL of 5% KOH aqueous solution at boil under vigorous stirring for 6 h. The suspension was kept under stirring at room temperature for another 12 h, filtered and washed with water. The solid was bleached in 150 mL of 1.7% $NaClO_2$ in pH 4 acetate buffer at 80 °C for 2 h, filtered and bleached with fresh reagents under the same condition for another 2 h, then filtered and washed with water. The solid was re-suspended in 150 mL of 5% KOH for 48 h then centrifuged to collect the purified chitin.

Chitin whiskers (CtNWs) were prepared by hydrolyzing the purified chitin with 3 N HCl at *ca.* 30 mL/g HCl/chitin ratio under stirring at boil for 90 min. The reaction was stopped by adding 50 mL of water and centrifuged (3400 rpm for 15 min). The precipitate was re-suspended in *ca.* 200 mL of water then centrifuged and repeated three times. The precipitate was re-suspended in water, dialyzed until neutral pH, then adjusted to pH 3 using 1 N HCl. The suspension was sonicated (Misonix, ultrasonic liquid processors, model CL5, USA) for a total of 20 min with 5 min of interval between every 5 min of sonication. The suspension was kept at 8 °C. The yield of chitin whiskers was determined by gravimetric analysis, in triplicate. The solid residue of 1000 μL sample oven-dried at 50 °C was correlated to the total volume of the whiskers suspension.

2.3. Surface deacetylation of CtNWs

Chitosan-sheath chitin-core whiskers (CsNWs) were obtained by the deacetylation of never-dried CtNWs suspension with 50 wt% NaOH at 50 °C for 48 h. The suspension was diluted with water and centrifuged at 5000 rpm for 10 min, then the supernatant decanted. This process was repeated 3 times. The sample was dialyzed in water to reach neutral pH, adjusted to pH 3 by 1 N HCl, and then homogenized by sonication.

2.4. Characterization

Characterization of CtNWs and CsNWs was performed on never-dried suspensions as well as freeze-dried or air-dried samples, depending on the technique used. Zeta potential measurements were performed on never-dried suspensions of CtNWs or CsNWs. Individual nanowhiskers were observed by transmission electron microscopy by air-drying aqueous suspension on appropriate surface. For scanning electron microscopy and X-ray diffraction, CtNWs (1.38 w/v%) and CsNWs (0.48 w/v%) suspensions were dried by freezing in liquid nitrogen (*ca.* −196 °C) and freeze-dried for 3 days (−50 °C and 0.12 mbar, Labconco Free zone dry system, USA).

2.4.1. Zeta potential

Zeta potential was measured using a ZetaSizer (nano ZS90, Malvern) with an autotitrator (MPT-2). Both CtNWs and CsNWs suspensions were diluted to 0.1 wt% using HCl solution at pH *ca.* 1. The zeta potential values of each sample was collected over the pH range from 1 to 12 using 0.5 N NaOH as the titrate.

2.4.2. Transmission electron microscopy (TEM)

8 μL of 0.01% CtNWs or CsNWs suspensions were deposited onto glow-discharged carbon-coated TEM grids (300-mesh copper, formvar-carbon, Ted Pella Inc., Redding, CA) and the excess liquid was removed by blotting with a filter paper. The specimens were then negatively stained with 2% uranyl acetate solution for 5 min, blotted with a filter paper to remove excess staining solution and allowed to dry under ambient condition. The samples were observed using a Philip CM12 transmission electron microscope operating at accelerating voltage of 100 kV. The average length of nanocrystals was calculated from measurements over 200 samples using analySIS FIVE software.

2.4.3. X-ray diffraction (XRD)

XRD spectra were collected on a Scintag XDS 2000 powder diffractometer using a Ni-filtered Cu Kα radiation (λ = 1.5406 Å) at an anode voltage of 45 kV and a current of 40 mA. Freeze-dried samples were pressed between two glass slides into 1-mm thick flat sheets. XRD patterns were recorded in a range of 2θ from 5° to 40° at a scan rate of 2°/min. The crystallinity (*CrI*, %) was calculated by:

$$CrI = \frac{A_C}{A_T} \times 100 \quad (1)$$

where A_C is the total area under the crystalline diffraction peaks and A_T is the total area under the curve in the 2θ range of 5°–30°. The XRD spectra was resolved into individual peaks, smoothed using 10 points in a second-order regression based on Savitzky–Golay filter and then deconvoluted based on Gaussian or Lorentzian functions in the Origin software release 8.5.

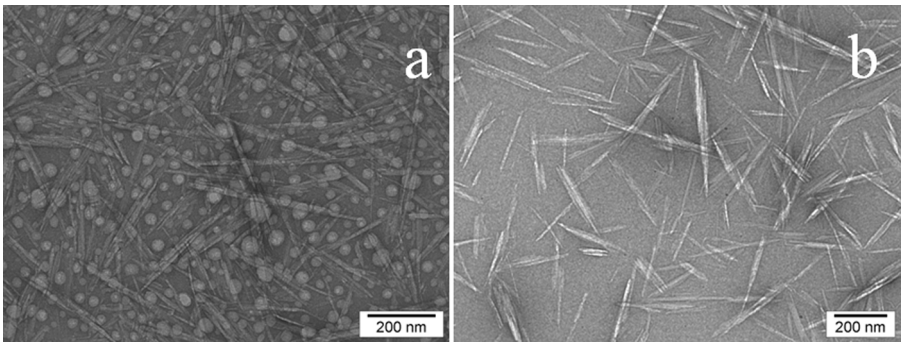

Fig. 1. TEM images of (a) acid hydrolyzed chitin (CtNWs, 3 N HCl, 90 min at boil) and (b) chitosan (CsNWs, 50% NaOH, 50 °C, 48 h) nanocrystals.

2.4.4. ^{1}H NMR, 2D HSQC NMR, and ^{13}C NMR

Solvent exchange was performed by pouring 10 mL of aqueous CtNWs (1.38 w/v%) or CsNWs (0.48 w/v%) suspensions into acetone to reach a 15/1 v/v acetone/H_2O ratio. The precipitate was recovered by centrifugation (5000 rpm, 10 min) and the supernatant decanted. CtNWs or CsNWs were re-suspended in 50 mL of acetone followed by centrifugation, using the same time and speed parameters as above, discharging the supernatant. This process was repeated 3 times. Then, specific amount of CtNWs or CsNWs was suspended in 1 mL of D_2O to form a colloidal suspension, and heated at 30 °C under vacuum for 2 h to remove the remaining acetone. The sample was left covered with highly porous tissue paper overnight under ambient condition before NMR acquisition. ^{1}H, ^{13}C, and 2D HSQC (Heteronuclear Single Quantum Coherence) NMR were conducted with a Bruker NMR spectrometer (800 MHz) using 5 mm CPTCI ^{1}H–^{13}C/15 N/D Z-GRD probe. ^{1}H NMR spectra were obtained at 303 K in deuterated oxide (99.9% D) as solvent with zgpr standard parameter set with 16 scans and 2 dummy scans). ^{13}C NMR and 2D HSQC experiments were obtained with respectively zgdc (14,368 scans and 2 dummy scans) and hsqcetqp (64 scans and 16 dummy scans) standard sets. For comparison, ^{1}H NMR spectrum of freeze-dried CsNWs dissolved in 2% deuterated acetic acid (CD_3COOD) in D_2O was obtained using the same parameters described previously.

3. Results and discussion

Pure chitin was obtained by alkaline treatment (5% KOH, 6 h at boil, 12 h at room temperature) and bleaching (1.7% $NaClO_2$, pH 4, 80 °C, 2 h) of practical grade crab shell chitin to 75% yield (Pereira et al., 2014). Purified chitin was hydrolyzed with HCl to cleavage the glycosidic linkages in the less ordered regions to produce highly crystalline (86% *CrI*) chitin nanowhiskers (CtNWs) at 65% yield from the purified chitin or 49% of commercially available chitin. CtNWs were surface deacetylated with 50 wt% NaOH at 50 °C to chitosan-sheath and chitin-core nanowhiskers (CsNWs) at 74% yield of CtNWs.

TEM (Fig. 1) images reveal both CtNWs and CsNWs to be rod-like and similar in widths and lengths, *i.e.*, 16 (±5.2) nm and 214 (±49) nm for CtNWs and 15 (±5.4) nm and 247 (±88) nm for CsNWs, respectively. Deacetylation did not alter their overall rod-like morphology nor dimensions significantly, but caused 26% mass loss. The slightly increased average length and, in particular, its standard deviation suggest the loss to be attributed to the dissolution of smallest nanowhiskers from hydrolysis. It should be noted that the spherical forms observed in Fig. 1a were artifacts from staining.

Chitin is usually not fully acetylated due to the purification processes. Even if CtNWs are 100% acetylated, complete deacetylation of 100% acetylated chitin to chitosan would lead to 21% mass reduction (*i.e.*, 42 g/mole of acetyl amide to amine out of 202 g/mole). Acid hydrolysis or deacetylation of CtNWs is thought to occur on the surface, thus is expected to cause less than the 21% mass loss. Therefore, the 26% mass loss was attributed to a combination of surface deacetylation of chitin nanorods and dissolution of small rods into soluble oligomers, monomers and acetic acid. As the suspensions consisting the deacetylated products were recovered following several purification steps (*e.g.* centrifugation, dialysis, *etc.*), as described in Section 2, these soluble products were not present in the samples used for all the following analysis.

Zeta potentials of CtNWs and CsNWs showed similar profiles over nearly full range of pH, *i.e.*, positively charged under acid conditions, decreasing charges to zero, and then becoming negatively charged under basic conditions (Fig. 2). However, CsNWs were more positively charged under acidic conditions (~+40 mV at pH range 3–6) and less negatively charged under basic conditions (~−15 mV at pH > 9) than CtNWs (~+30 mV and −25 mV, respectively). The pHs where the nanowhiskers carry zero charges or the isoelectric points (IPs) were pH 7.3 and pH 8.8 for CtNWs and CsNWs, respectively. The higher zeta potentials of CsNWs at low pHs is consistent with protonation of amine, $R\text{-}NH_2 + H_3O^+ \leftrightarrow R\text{-}NH_3^+ + H_2O$. The negative zeta potentials for both CtNWs and CsNWs under basic conditions are due to the association of OH^- from the NaOH titrant to the slipping plane of the colloid. The higher IP of CsNWs than that of CtNWs results from the higher consumption of added OH^- to neutralize the colloid charges during titration. Similarly, more OH^- groups are attached to the CtNWs slipping plane than to CsNWs leading to the higher negative zeta potentials of CtNWs under the same basic conditions. The fact that

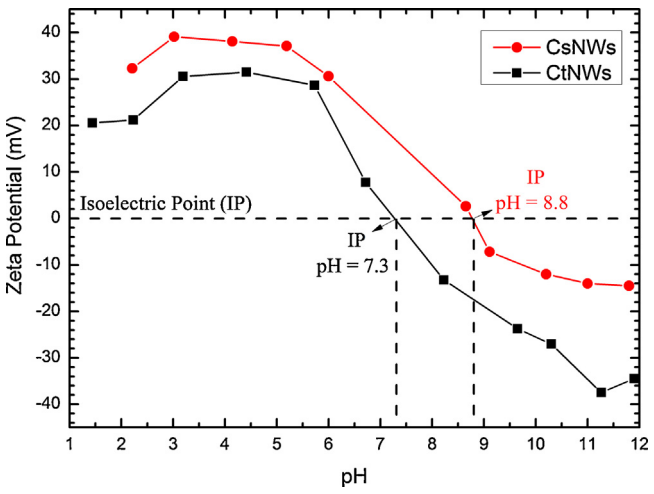

Fig. 2. Zeta Potential measurements *versus* pH of acid hydrolyzed chitin (CtNWs, 3 N HCl, 90 min at boil) and chitosan (CsNWs, 50% NaOH, 50 °C, 48 h) nanocrystals (at 0.1 wt%). Isoelectric point (IP) is indicated.

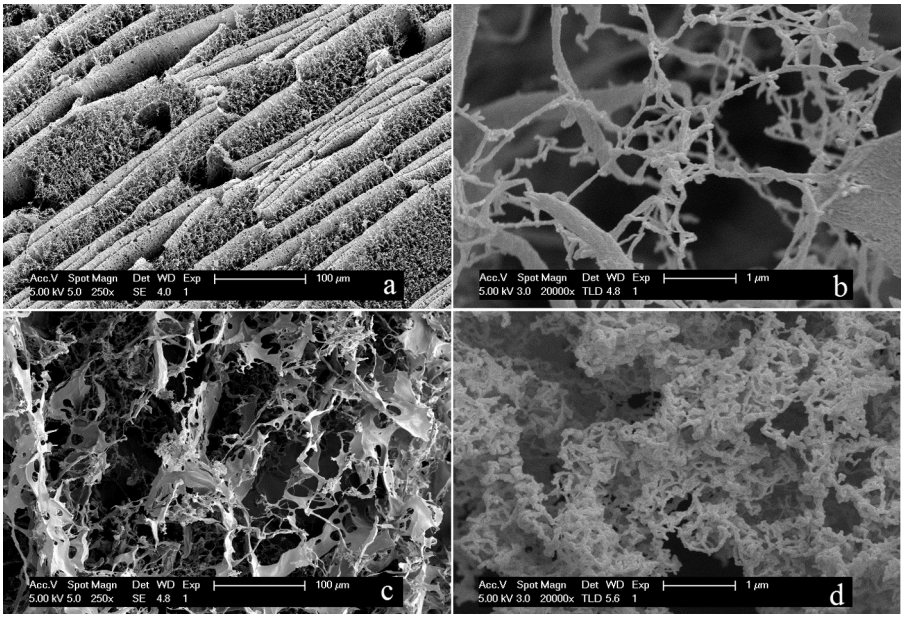

Fig. 3. Self-assembling effect upon drying: SEM images of freeze-dried (a) and (b) chitin (CtNWs) and (c) and (d) chitosan (CsNWs) nanocrystals.

CtNWs are positively charged at acidic pH indicates the presence of some surface amines. In other words, the CtNW surfaces are not completely acetylated. Deacetylation converts the more accessible surface acetylamide ($-NHC(O)CH_3$) to amine ($-NH_2$) which are more positively charged at low pHs.

Rapid freezing dilute aqueous suspensions (~1 wt%, at pH 3) of either CtNWs or CsNWs in liquid nitrogen (−196 °C) followed by freeze-drying (−50 °C) produced white fluffy mass in both cases. The rapidly frozen and freeze-dried CtNWs appeared as tens of micrometer thick sheets predominantly, interconnected with webs of much smaller (<100 nm wide) fibrils (Fig. 3a and b). CsNWs, on the other hand, assembled into predominantly fibrillar structures with some thin film-like pieces (with varied lengths from few to tens of micrometers and width of 36 ± 8 μm). Since CtNWs and CsNWs have similar dimensions and size distributions, the distinct morphologies observed reflect the effects of their different surface chemistries. The surface deacetylated CsNWs are more highly positively charged from protonated amine groups than the slightly surface deacetylated CtNWs, as shown by zeta potential. At pH 3, the more positively charged CsNWs have higher repulsive forces to remain segregated during freezing, leading to *ca.* 100 nm fibrillar form upon lyophilization. That few similarly appearing fibrils also observed from freeze drying of CtNWs indicate the presence of some more deacetylated CtNWs that behave more like CsNWs. Upon rapid freezing with liquid nitrogen, immediate ice nucleation and crystallization concentrate the nanowhiskers to close proximities, leading to their aggregation enforced by hydrogen-bonds among surface functional groups *e.g.*, hydroxyl (—OH), acetylamide ($-NHC(O)CH_3$) and amine ($-NH_2$) but balanced by the electrostatic repulsive forces of protonated amines ($-NH_3^+$). Therefore, the different assembled structures observed for CtNWs and CsNWs are exclusively related to the different surface chemistries from deacetylation and as a result depends on the balance between the electrostatic repulsive forces and the attractive H-bonds among nanocrystals. In other words, as CsNWs have more deacetylated surface layers, the electrostatic repulsive forces caused by the positively charged groups at CsNWs predominates over H-bonds leading to a less ordered fibrillar structure upon drying while H-bonds play stronger role to assemble the more acetylated CtNWs into a more compact and ordered structure.

Chitosan is the linear cationic (1-4)-2-amino-2-deoxy-β-D-glucan industrially produced from marine chitin (Muzzarelli, Mehtedi, & Mattioli-Belmonte, 2014; Muzzarelli, 2010, 2012) Conventionally, chitin/chitosan are named according to their degree of acetylation (DA), *i.e.*, chitin has DA ≥ 50% whereas chitosan has DA < 50% (Gonil & Sajomsang, 2012). However, CsNWs have the surface layers deacetylated while the core remained acetylated, so chitosan-sheath chitin core nanowhisker is the more appropriate term.

The XRD of CtNWs (Fig. 4) presented diffraction peaks characteristics of α-chitin at $2\theta = 9.3°$, 19.1°, 20.7°, 23.1° and 26.2° associated with the (0 2 0), (1 1 0), (1 2 0), (1 3 0) and (0 1 3) crystallographic planes, respectively, and a CrI of 86%. CsNWs had the same XRD diffraction signals as CtNWs, but less intense at $2\theta = 9.3°$, broader and less resolved peak at 19.1° and a lower *CrI* of 54%. The 32% lower crystallinity of CsNWs is consistent with surface deacetylation of CtNWs. Assuming these nanowhiskers to be 100% crystalline in their cores and amorphous on their shells, *ca.* 93% and 74% of the lateral dimensions of CtNWs and CsNWs would be crystalline

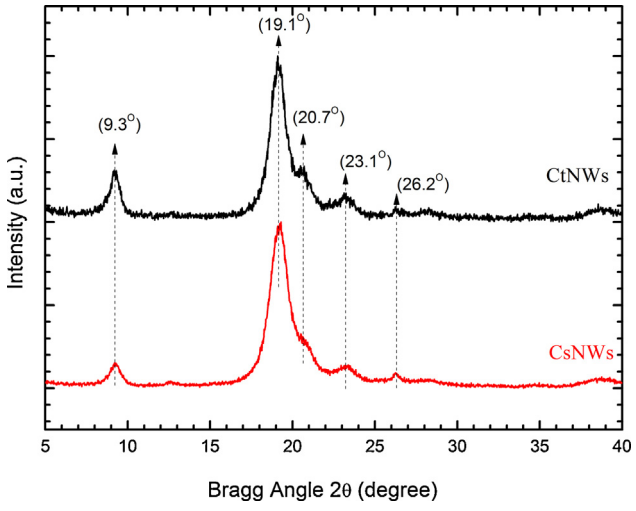

Fig. 4. XRD diffractograms of chitin (CtNWs) and chitosan (CsNWs) nanocrystals.

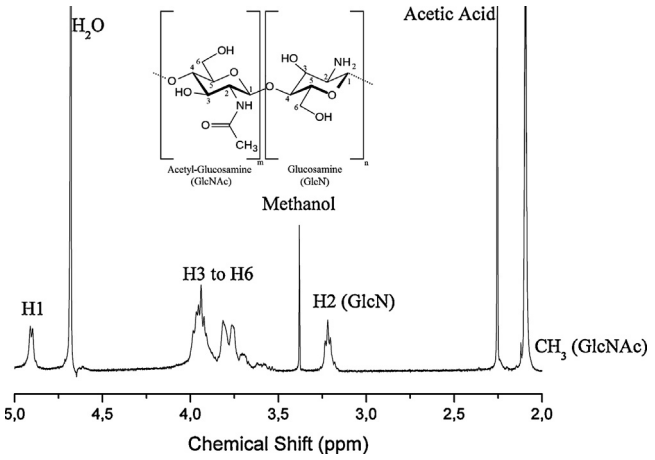

Fig. 5. ^{1}H NMR spectrum of solubilized chitosan nanocrystals (CsNWs, 50% NaOH, 50 °C, 48 h) in 2% CD_3COOD/D_2O. The inset shows the repeating unit of chitin ($m > n$) or chitosan ($m < n$).

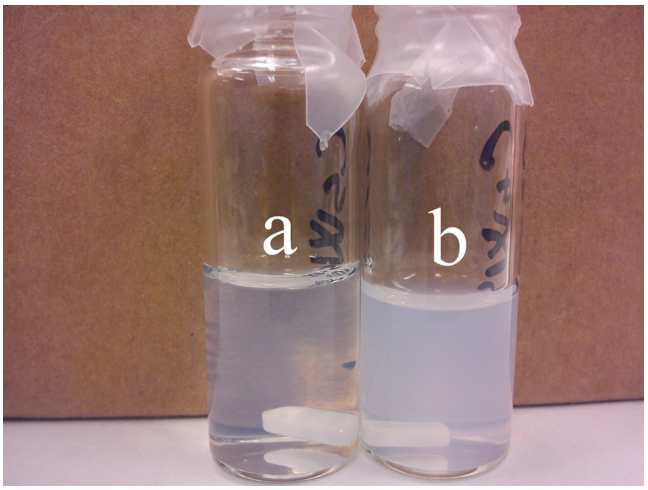

Fig. 6. Photograph of (a) chitosan (CsNWs) and (b) chitin (CtNWs) nanocrystals in D_2O for NMR acquisition.

based on their *CrI* values. In other words, *ca.* 7% and 26% outside radius of CtNWs and CsNWs are non-crystalline, respectively. The slightly non-crystalline surfaces of CtNWs are consistent with their partially deacetylated surfaces while the more extensively deacetylated CsNWs contain thicker amorphous surface layer that constitute the outer 26% of their radius.

^{1}H NMR spectrum of freeze-dried CsNWs dissolved in 2% deuterated acetic acid (CD_3COOD) in D_2O presented the characteristic soluble chitosan signals: δ 2.1 ppm from the three methyl H atoms (GlcNAc), δ 3.2 ppm from H2 (GlcN), several overlapping signals from δ 3.5 to 4.0 ppm from H3–H6 connected to the non-anomeric C3–C6 carbons in the glucopyranose ring and *ca.* δ 4.9 ppm from anomeric proton (Fig. 5). ^{1}H NMR spectrum of soluble chitosan as well as solid ^{13}C NMR have been extensively described in the scientific literature (de Alvarenga, Pereira de Oliveira, & Roberto Bellato, 2010; Hirai, Odani, & Nakajima, 1991; Kasaai, 2010; Rinaudo, 2006). This ^{1}H NMR spectrum of CsNWs dissolved in CD_3COOD is virtually the same as ^{1}H NMR extensively reported for soluble chitosan as well as solid ^{13}C NMR described in the scientific literature (de Alvarenga et al., 2010; Hirai et al., 1991; Kasaai, 2010; Rinaudo, 2006). This confirms CD_3COOD to be a good solvent for CsNWs and the spectrum represents that of solubilized CsNWs, not that of individualized nanocrystals.

As verified by SEM images, CtNWs and CsNWs can easily self-assemble during freeze-drying. Therefore, any characterization technique based on dried samples will provide information from the bulk of the sample rather than the surface of the individualized nanocrystals. Then, suspension preparation to maintain individual CtNWs and CsNWs for NMR acquisition is crucial to obtain well resolved and reliable data. Intermediate solvent exchange from aqueous medium to acetone was first performed to prevent association and aggregation of nanowhiskers in the process of removing water, which is not suitable for NMR acquisition. Acetone, chosen for its high volatility, was then removed from D_2O suspension by mild heating at 30 °C at reduced pressure. At *ca.* 0.1 wt% in D_2O, the CtNWs suspension appeared slightly more opalescent than CsNWs (Fig. 6) indicating CsNWs to be better dispersed in D_2O.

2D HSQC NMR is a very sensitive technique in liquid state that correlates chemical shifts of hetero bound nuclei. In ^{1}H–^{13}C HSQC the magnetization from ^{13}C is transferred to ^{1}H, improving the sensibility of ^{13}C (McKenzie, Charlton, Donarski, MacNicoll, & Wilson, 2010). ^{1}H–^{13}C HSQC from the solvent exchanged CsNWs correlates the hydrogen atom bonded to its respective carbon atom (Fig. 7). The ^{1}H–^{13}C correlation for H1/C1 appears at δ 4.5/100, those for H3–H6/C3–C6 are observed at δ 3.7–4.1 ppm/δ 70–83 ppm and the three methyl hydrogen atoms H/CH_3 appear at δ 2.1 ppm/δ 20–25 ppm. The carbon C2 signal at δ 50 ppm for GlcN shows two hydrogen correlations at δ 3.35 ppm and δ 3 ppm on the HSQC spectrum while the C2 from GlcNAc at δ 55 ppm corresponds to hydrogen at δ 2.75 ppm. The α-chitin chains in the orthorhombic crystals have shown inter-chains hydrogen bonding along the *a* axis through C═O···H—N between the acetylamide groups (—NHC(O)CH_3) of adjacent chains (Cho, Jang, Park, & Ko, 2000). Therefore, in partially deacetylated CsNWs, inter-chain interactions due to the crystalline chitin core could create different chemical environments for H2 atoms bonded to C2 (GlcN), splitting the signals in two, as observed in the HSQC (Fig. 7). In other words, different H-bond interactions between the proton donor (amine from glucosamine unit) and acceptor groups could be identified.

The ^{1}H–^{13}C HSQC data of CtNWs was obtained (not shown) with very poor resolution probably due to the high crystallinity of samples. However, as surface deacetylation took place and the *CrI* decreased from 86% to 54%, the surface chains of CsNWs became more mobile and susceptible to magnetization to generate resonance as observed in the spectra (Fig. 7). The significance of this observation is that NMR detects the more mobile surface chains of CsNWs in suspensions and is a powerful tool to assess chemical modification of these polysaccharide nanocrystal surfaces.

^{1}H NMR spectra (Fig. 8) of both solvent exchanged CtNWs and CsNWs show a peak at δ 2.20 ppm attributed to the three acetyl-glucosamine hydrogens, a signal at δ 3.35 ppm correlated to H2 from the glucosamine unit (carbon 2), several signals in the δ 3.50–δ 4.00 ppm range corresponding to the non-anomeric hydrogens H3–H6 from the ring and one at δ 4.60 ppm attributed to the hydrogen H1 connected to the anomeric carbon C1. All these signals presented similar chemical shifts from those observed for soluble chitosan (Fig. 5). However, new peaks, not observed on the soluble form of chitosan, appeared at δ 3.00 ppm and δ 2.75 ppm. In previously reported ^{1}H NMR (Lertwattanaseri et al., 2009; Phongying et al., 2006, 2007), the chitosan was over 95% deacetylated from chitin whiskers and prepared in 2 v% acetic acid for NMR analysis. Since chitosan dissolves in 2% acetic acid and the NMR data presented, specially the signal referring to H2 atoms bonded to C2 (GlcN) at *ca.* δ 3.2 ppm, were characteristic from soluble chitosan, not whiskers. Herein, the use of D_2O avoids any possible solubilization or damage to the crystalline structure of the nanowhiskers. Signals at δ 3.00 ppm and at δ 2.75 ppm are related to different chemical environments experienced by the H2 atoms in the crystalline structure of both CtNWs and CsNWs but not in the soluble

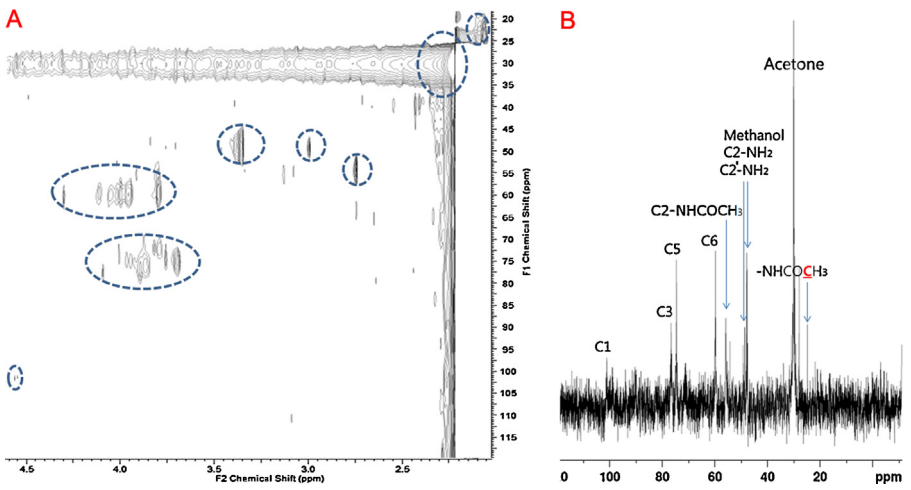

Fig. 7. (a) 2D HSQC and (b) ^{13}C NMR of chitosan (CsNWs) nanocrystals.

form. In the soluble form, the chitosan molecules are solvated by the solvent and its H2 atoms corresponding to the GlcN or GlcNAc residues have all the same chemical environment for each residue, presenting only one NMR signal; *e.g.* the NMR signal corresponding to H2 (GlcN) is located at *ca.* δ 3.2 ppm while the signal related to H2 (GlcNAc) is overlapped in the δ 3.5–4.0 ppm region. On the other hand, the glucosamine amine of CsNWs can H-bond to either amine or acetylamide group from adjacent chains to promotes distinct shielding effects on H2, generating the two signals at δ 3.00 ppm and at δ 3.35 ppm. Similarly, the acetylamide group (GlcNAc) can also interact distinctly depending on the adjacent chain generating the new signals in the region at δ 2.75 ppm.

Table 1 summarizes the ^{1}H–^{13}C HSQC and ^{1}H NMR assignments for CtNWs and CsNWs.

The degree of acetylation was also estimated from the ^{1}H NMR data by the integrals of the methyl proton in acetyl-glucosamine (GlcNAc) to that of H2 in glucosamine (GlcN) as:

$$\%DA = \left[\frac{(1/3I_{CH3})}{(I_{H2} + I_{H2'})} \times 100\right] \quad (2)$$

where I_{CH3} is the integral of methyl proton (GlcNAc) and $I_{H2} + I_{H2'}$ is the sum of integrals of proton connected to C2 in GlcN. Using deuterated methanol as the internal standard for calculating the integrals, the calculated DA for CtNWs and CsNWs was 56% and 9%, respectively. Such DA values are associated with the surface layers since both CtNWs and CsNWs have highly crystalline chitin core. As presented earlier, 93% and 74% of their respective radius to be crystalline core based on 86% and 54% *CrI* values for CtNWs and CsNWs, respectively. These NMR derived DA data indicate that 44% of the thin surface layer (7% of the radius) of CtNWs and 93% of the much thicker outer portion (26% of the radius) of CsNWs are deacetylated. Therefore, by using ^{1}H NMR measurements was possible to verify subtle distinction of the chemical environments of H2 atoms of both CtNWs and CsNWs which presented chemical shifts at δ 2.75 ppm and at δ 3.00 that were not present in the soluble form of chitosan. Furthermore, the degree of acetylation at the nanocrystals surfaces was monitored by employing the integrals of such signals according to Eq. (2). Then, ^{1}H NMR may be a powerful tool in discerning surface structures of chemically modified CtNWs and CsNWs for potential functionalization of CtNWs and CsNWs for further applications.

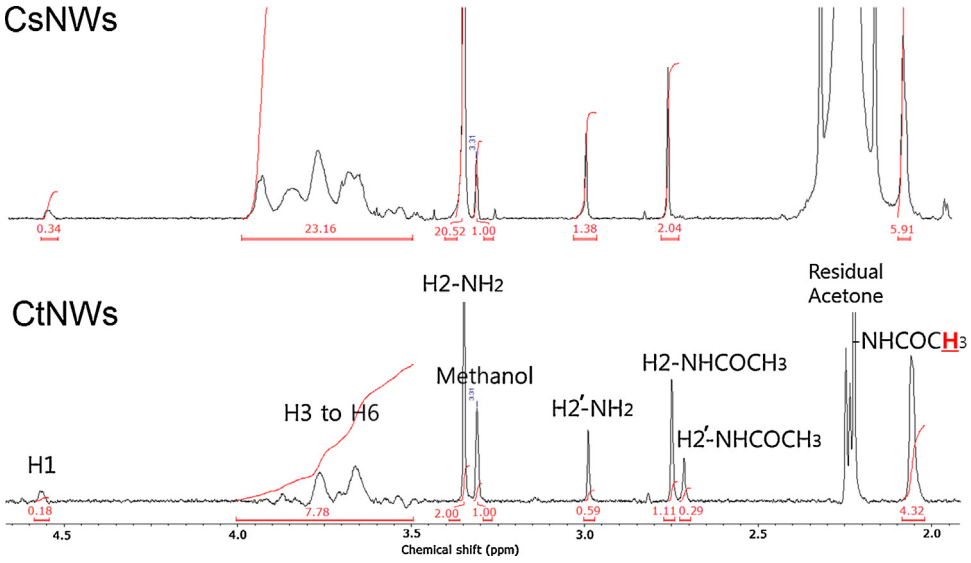

Fig. 8. ^{1}H NMR spectra of chitin (CtNWs) and chitosan (CsNWs) nanocrystals.

Table 1
Assignments of ^{1}H and ^{13}C chemical shifts (δ) for CtNWs and CsNWs obtained in D_2O and 2% CD_3COOD.

^{1}H–^{13}C HSQC CsNWs[a]		^{1}H NMR CtNWs[a]	^{1}H NMR CsNWs[a]	^{1}H NMR CsNWs[b]	
(δ_H/δ_C, ppm)	Assignment	(δ_H, ppm)	(δ_H, ppm)	(δ_H, ppm)	Assignment
2.1/25	—CH_3 (GlcNAc)	2.05	2.1	2.1	—CH_3
4.6/100	H1/C1 (anomeric)	4.55	4.5	4.9	H1
3.7–4.1/70–83	H3–H6/C3–H6	3.5–4.0	3.5–4.0	3.5–4.0	H3–H6
3.35/50	H2/C2 (GlcN)	2.75	2.75	–	H2 (GlcNAc)
3/50	H2′/C2 (GlcN)	2.7	–	–	H2′ (GlcNAc)
2.75/55	H2/C2 (GlcNAc)	3.35	3.35	3.2	H2 (GlcN)
		3.0	3.0	–	H2′ (GlcN)

[a] Spectra obtained from never dried suspensions prepared in D_2O.
[b] Spectrum obtained from dissolution of CsNWs in 2% deuterated acetic acid in D_2O.

4. Conclusions

This paper reports consistent surface characterization of chitin/chitosan nanowhiskers in the never-dried state using liquid-state high-resolution NMR. Chitin nanowhiskers (CtNWs) were isolated from chitin by acid hydrolysis (3 N HCl, 30 mL/g, 104 °C) at 65% yield of chitin and then surface deacetylated (50% NaOH, 48 h, 50 °C) to generate chitosan-sheath chitin core nanowhiskers (CsNWs) at 74% yield of CtNWs. Surface deacetylation of CtNWs to CsNWs was clearly evident by the zeta potentials, showing increase in IP value from 7.3 to 8.8 as well as the increase in positive charges at acid condition and decrease of negative charges at basic condition. Although the rod-like morphology and the average dimensions (15 ± 5.4 nm wide and 247 ± 88 nm long) remained essentially the same for CsNWs, deacetylation caused a significant 32% reduction in crystallinity to 54%. Solvent exchange from H_2O to acetone then to D_2O was critical and effective to prevent clustering of both CtNWs and CsNWs for NMR measurements of individual nanowhiskers. The crystalline cores of CtNWs and CsNWs provides different chemical environments for the hydrogen atom H2 (glucosamine unit) splitting the NMR signals into 2 (δ 3.0 and δ 3.35 ppm) distinct from that observed for the soluble form of chitosan (δ 3.2 ppm). Besides, ^{1}H–^{13}C HSQC was only possible for CsNWs indicating the NMR phenomenon observed represents only the less crystalline and more mobile outer surface layers. Therefore, NMR is a powerful technique to assess surface modifications of chitin whiskers.

Acknowledgments

The CAPES doctorate's fellowship (Process BEX 2394/11-1) and technical assistance of Drs. F. Jiang and B.K. Ahn on TEM, SEM, XRD and NMR are greatly appreciated.

References

Balogh, L. P. (2010). Why do we have so many definitions for nanoscience and nanotechnology? *Nanomedicine: Nanotechnology Biology and Medicine*, *6*(3), 397–398.
Bhattacharya, R., & Mukherjee, P. (2008). Biological properties of naked metal nanoparticles. *Advanced Drug Delivery Reviews*, *60*(11), 1289–1306.
Cárdenas, G., Cabrera, G., Taboada, E., & Miranda, S. P. (2004). Chitin characterization by SEM, FTIR, XRD, and ^{13}C cross polarization/mass angle spinning NMR. *Journal of Applied Polymer Science*, *93*(4), 1876–1885.
Cho, Y.-W., Jang, J., Park, C. R., & Ko, S.-W. (2000). Preparation and solubility in acid and water of partially deacetylated chitins. *Biomacromolecules*, *1*(4), 609–614.
de Alvarenga, E. S., Pereira de Oliveira, C., & Roberto Bellato, C. (2010). An approach to understanding the deacetylation degree of chitosan. *Carbohydrate Polymers*, *80*(4), 1155–1160.
Fan, Y., Saito, T., & Isogai, A. (2007). Chitin nanocrystals prepared by TEMPO-mediated oxidation of α-chitin. *Biomacromolecules*, *9*(1), 192–198.
Fan, Y., Saito, T., & Isogai, A. (2009). TEMPO-mediated oxidation of β-chitin to prepare individual nanofibrils. *Carbohydrate Polymers*, *77*(4), 832–838.
Fan, Y., Saito, T., & Isogai, A. (2010). Individual chitin nano-whiskers prepared from partially deacetylated α-chitin by fibril surface cationization. *Carbohydrate Polymers*, *79*(4), 1046–1051.
Faramarzi, M. A., & Sadighi, A. (2013). Insights into biogenic and chemical production of inorganic nanomaterials and nanostructures. *Advances in Colloid and Interface Science*, *189–190*, 1–20.
Gonil, P., & Sajomsang, W. (2012). Applications of magnetic resonance spectroscopy to chitin from insect cuticles. *International Journal of Biological Macromolecules*, *51*(4), 514–522.
Goodrich, J. D., & Winter, W. T. (2006). α-chitin nanocrystals prepared from shrimp shells and their specific surface area measurement. *Biomacromolecules*, *8*(1), 252–257.
Hirai, A., Odani, H., & Nakajima, A. (1991). Determination of degree of deacetylation of chitosan by ^{1}H NMR spectroscopy. *Polymer Bulletin*, *26*(1), 87–94.
Huang, Y., Zhang, L., Yang, J., Zhang, X., & Xu, M. (2013). Structure and properties of cellulose films reinforced by chitin whiskers. *Macromolecular Materials and Engineering*, *298*(3), 303–310.
Jiang, F., & Hsieh, Y.-L. (2013). Chemically and mechanically isolated nanocellulose and their self-assembled structures. *Carbohydrate Polymers*, *95*(1), 32–40.
Kasaai, M. R. (2010). Determination of the degree of N-acetylation for chitin and chitosan by various NMR spectroscopy techniques: A review. *Carbohydrate Polymers*, *79*(4), 801–810.
Lertwattanaseri, T., Ichikawa, N., Mizoguchi, T., Tanaka, Y., & Chirachanchai, S. (2009). Microwave technique for efficient deacetylation of chitin nanowhiskers to a chitosan nanoscaffold. *Carbohydrate Research*, *344*(3), 331–335.
Marchessault, R. H., Morehead, F. F., & Walter, N. M. (1959). Liquid crystal systems from fibrillar polysaccharides. *Nature*, *184*, 632–633.
McKenzie, J., Charlton, A., Donarski, J., MacNicoll, A., & Wilson, J. (2010). Peak fitting in 2D ^{1}H–^{13}C HSQC NMR spectra for metabolomic studies. *Metabolomics*, *6*(4), 574–582.
Muzzarelli, R., Mehtedi, M., & Mattioli-Belmonte, M. (2014). Emerging biomedical applications of nano-chitins and nano-chitosans obtained via advanced eco-friendly technologies from marine resources. *Marine Drugs*, *12*(11), 5468–5502.
Muzzarelli, R. A. A. (2010). Chitins and chitosans as immunoadjuvants and non-allergenic drug carriers. *Marine Drugs*, *8*(2), 292–312.
Muzzarelli, R. A. A. (2012). 10.06 – Nanochitins and nanochitosans, paving the way to eco-friendly and energy-saving exploitation of marine resources. In K. M. Möller (Ed.), *Polymer science: A comprehensive reference* (pp. 153–164). Amsterdam: Elsevier.
Paillet, M., & Dufresne, A. (2001). Chitin whisker reinforced thermoplastic nanocomposites. *Macromolecules*, *34*(19), 6527–6530.
Pereira, A. G. B., Muniz, E. C., & Hsieh, Y.-L. (2014). Chitosan-sheath and chitin-core nanowhiskers. *Carbohydrate Polymers*, *107*, 158–166.
Phongying, S., Aiba, S.-I., & Chirachanchai, S. (2006). A novel soft and cotton-like chitosan-sugar nanoscaffold. *Biopolymers*, *83*(3), 280–288.
Phongying, S., Aiba, S.-I., & Chirachanchai, S. (2007). Direct chitosan nanoscaffold formation via chitin whiskers. *Polymer*, *48*(1), 393–400.
Rinaudo, M. (2006). Chitin and chitosan: Properties and applications. *Progress in Polymer Science*, *31*(7), 603–632.
Thakkar, K. N., Mhatre, S. S., & Parikh, R. Y. (2010). Biological synthesis of metallic nanoparticles. *Nanomedicine: Nanotechnology, Biology, and Medicine*, *6*(2), 257–262.
Xia, Y., Xiong, Y., Lim, B., & Skrabalak, S. E. (2009). Shape-controlled synthesis of metal nanocrystals: simple chemistry meets complex physics? *Angewandte Chemie International Edition*, *48*(1), 60–103.
Zeng, J.-B., He, Y.-S., Li, S.-L., & Wang, Y.-Z. (2011). Chitin whiskers: An overview. *Biomacromolecules*, *13*(1), 1–11.